

# Does a Neural Network Really Encode Symbolic Concept?

Mingjie Li Quanshi Zhang\*

Shanghai Jiao Tong University

## Abstract

Recently, a series of studies have tried to extract interactions between input variables modeled by a DNN and define such interactions as concepts encoded by the DNN. However, strictly speaking, there still lacks a solid guarantee whether such interactions indeed represent meaningful concepts. Therefore, in this paper, we examine the trustworthiness of interaction concepts from four perspectives. Extensive empirical studies have verified that a well-trained DNN usually encodes sparse, transferable, and discriminative concepts, which is partially aligned with human intuition. *The code will be released when the paper is accepted.*

## 1. Introduction

Understanding the black-box representation of deep neural networks (DNNs) has received increasing attention in recent years. Unlike graphical models with interpretable internal logic, the layerwise feature processing in DNNs makes it naturally difficult to explain DNNs from the perspective of symbolic concepts. Instead, previous studies interpreted DNNs from other perspectives, such as illustrating the visual appearance that maximizes the inference score [Simonyan et al., 2013, Yosinski et al., 2015], and estimating attribution/importance/saliency of input variables [Ribeiro et al., 2016, Sundararajan et al., 2017, Lundberg and Lee, 2017a]. Zhou et al. [2015], Bau et al. [2017], Kim et al. [2018] visualized the potential correspondence between convolutional filters in a DNN and visual concepts in an empirical manner.

**Unlike previous studies, a series of studies [Ren et al., 2021, 2023, Deng et al., 2022] tried to define and propose an exact formulation for the concepts encoded by a DNN.** Specifically, these studies discovered that a well-trained DNN usually encoded various interactions between different input variables, and the inference score on a specific input sample could be explained by numerical effects of different interactions. Thus, they claimed that each interaction pattern was a symbolic concept encoded by the DNN.

\*Quanshi Zhang is the corresponding author. He is with the Department of Computer Science and Engineering, the John Hopcroft Center, at the Shanghai Jiao Tong University, China. [zqs1022@sjtu.edu.cn](mailto:zqs1022@sjtu.edu.cn)

Specifically, let us consider a DNN given a sample with  $n$  input variables  $N = \{1, 2, \dots, n\}$  e.g., given a sentence with five words “*he is a green hand.*” The DNN usually does not use each individual input variable for inference independently. Instead, the DNN lets different input variables interact with each other to construct concepts for inference. For example, a DNN may memorize the interaction between words in  $S = \{\text{green}, \text{hand}\}$  with a specific numerical contribution  $I(S)$  to push the DNN’s inference towards the meaning of a “*beginner.*” Such a combination of words is termed an *interaction concept*. Each interaction concept  $S \subseteq N$  represents the AND relationship between input variables in  $S$ . Only the co-appearance of input variables in  $S$  can make an interaction effect  $I(S)$  on the network output. In contrast, masking any word in  $\{\text{green}, \text{hand}\}$  removes the interaction effect  $I(S)$ . In this way, Ren et al. [2021] proved that the inference score  $y$  of a trained DNN on each sample can be written as the sum of effects of all potential symbolic concepts  $S \subseteq N$ , i.e.  $y = \sum_{S \subseteq N} I(S)$ .

*However, the claim that “a DNN encodes symbolic concepts” is too counter-intuitive. Ren et al. [2021] just formulated  $I(S)$  that satisfied  $y = \sum_{S \subseteq N} I(S)$ . Current studies have not provided sufficient support for the claim that a DNN really learns symbolic concepts. In fact, we should not ignore another potential situation that the defined effect  $I(S)$  is just a mathematical transformation that ensures the decomposition of network output into concepts  $y = \sum_{S \subseteq N} I(S)$ , rather than faithfully representing a meaningful and transferable concept learned by a DNN.*

Therefore, in this paper, we aim to give a quantitative verification of the concept-emerging phenomenon, i.e., whether a well-trained DNN summarizes transferable symbolic knowledge from chaotic raw data, like what human brain does. Or the defined effect  $I(S)$  is just a mathematical game without clear meanings. To this end, we believe that if a well-trained DNN really encodes certain concepts, then the concepts are supposed to satisfy the following four requirements.

- **Representing network inference using a few concepts.** If a DNN really learns symbolic concepts, then the DNN’s inference on a specific sample is supposed to be concisely explained by a small number of salient concepts, rather than a large number of concepts, according to both

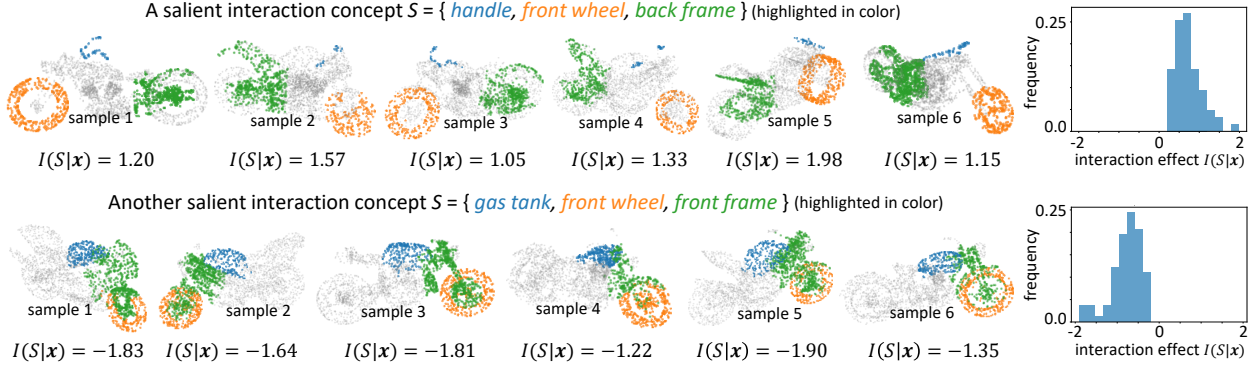


Figure 1. Visualization of interaction concepts  $S$  extracted by PointNet on different samples in the ShapeNet dataset. The histograms show the distribution of interaction effects  $I(S|x)$  over samples in the “motorbike” category, where  $S$  is extracted as a salient concept.

Occam’s Razor and people’s intuitive understanding towards concepts. In fact, the sparsity of concepts in a specific sample has been discussed by Ren et al. [2021]. In this paper, we further conduct extensive experiments on more diverse DNNs, in order to verify that a well-trained DNN usually extracts sparse concepts from each sample for inference.

- **A transferable concept dictionary through different samples.** If a DNN can use a relatively small set  $D$  of salient concepts, namely a concept dictionary, to approximate inference scores on different samples in a category, *i.e.*,  $\forall x, y \approx \sum_{S \in D} I(S|x)$ , then we consider the concept dictionary  $D$  represents common features shared by different samples in the category. Otherwise, if Ren et al. [2021] extract a fully different set of concepts from each different sample in the same category, then these concepts probably represent noisy signals. In other words, convincing concepts must be stably extracted with high transferability through different samples in the same category.

- **Transferability of concepts across different DNNs.** Similarly, when we train different DNNs for the same task, different DNNs probably learn similar sets of concepts if they really memorize the defined “concepts” as basic inference patterns for the task.

- **Discrimination power of concepts.** Furthermore, if a DNN learns meaningful concepts, then these concepts are supposed to exhibit certain discrimination power in the classification task. The same concept extracted from different samples needs to consistently push the DNN towards the classification of a certain category.

To this end, we conducted experiments on various DNNs trained on different datasets for classification tasks, including tabular datasets, image datasets, and point-cloud datasets. We found that all these trained DNNs encoded transferable concepts. On the other hand, we also investigated a few extreme cases, in which the DNN either collapsed into simple linear models or failed to learn transferable and discriminative concepts. In sum, although we cannot theoretically

prove the phenomenon of the emergence of transferable concepts, this phenomenon indeed happened for most tasks in our experiments.

**Contributions** of this paper can be summarized as follows. (1) Besides the sparsity of concepts, we propose three more perspectives to examine the concept-emerging phenomenon of a DNN, *i.e.*, whether the DNN summarizes transferable symbolic knowledge from chaotic raw data. (2) Extensive empirical studies on various tasks have verified that a well-trained DNN usually encodes transferable interaction concepts. (3) We also discussed three extreme cases, in which a DNN is unlikely to learn transferable concepts.

## 2. Related works

**Understanding the black-box representation of DNNs.** Many explanation methods have been proposed to explain DNNs from different perspectives. Typical explanation methods include visualizing patterns encoded by a DNN [Simonyan et al., 2013, Zeiler and Fergus, 2014, Yosinski et al., 2015, Dosovitskiy and Brox, 2016], estimating the attribution/importance/saliency of each input variable [Ribeiro et al., 2016, Sundararajan et al., 2017, Lundberg and Lee, 2017b, Fong and Vedaldi, 2017, Zhou et al., 2016, Selvaraju et al., 2017], and learning feature vectors potentially correspond to semantic concepts [Kim et al., 2018]. Some studies explained a DNN by distilling the network into another interpretable model [Frosst and Hinton, 2017, Che et al., 2016, Wu et al., 2018, Zhang et al., 2018, Vaughan et al., 2018, Tan et al., 2018]. However, most explanation methods did not try to disentangle concepts encoded by a DNN.

**Interaction encoded by DNNs.** Many recent studies have focused on quantifying interactions between input variables learned by a DNN [Sorokina et al., 2008, Murdoch et al., 2018, Singh et al., 2018, Jin et al., 2019, Janizek et al., 2020]. In game theory, Grabisch and Roubens [1999], Sundararajan et al. [2020], Tsai et al. [2022] proposed in-

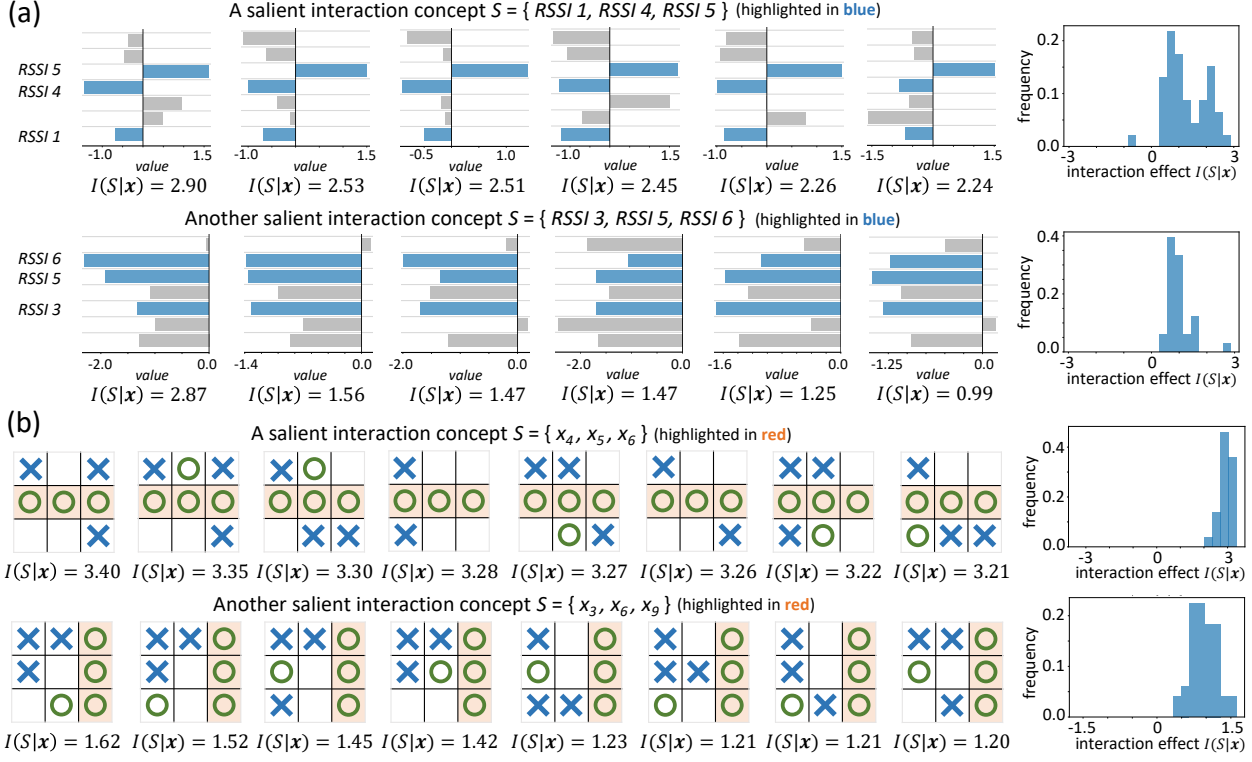


Figure 2. Visualization of interaction concepts  $S$  extracted by two *MLP-5* networks<sup>3</sup>, which are trained on (a) the *wifi* dataset<sup>3</sup> and (b) the *tic-tac-toe* dataset<sup>3</sup>. The histograms show (a) the distribution of interaction effects  $I(S|x)$  over samples in the 4<sup>th</sup> category, and (b) the distribution of interaction effects  $I(S|x)$  over samples in sub-categories<sup>4</sup> with patterns  $x_4 = x_5 = x_6 = 1$  and  $x_3 = x_6 = x_9 = 1$ .

teraction metrics from different perspectives. Recently, Ren et al. [2021] defined concepts encoded by a DNN as the interaction between input variables. Ren et al. [2023] further optimized baseline values of input variables based on such concepts. Besides, Deng et al. [2022] found that DNNs were less likely to encode interaction concepts of intermediate complexity. However, strictly speaking, there still lacks theoretical guarantee for the interaction to really represent concepts. Therefore, in this paper, we examine the trustworthiness of the interaction concepts from four perspectives.

### 3. Emergence of transferable concepts

#### 3.1. Preliminaries: representing network inferences using interaction concepts

It is widely believed that the learning of a DNN can be considered as a regression problem, instead of explicitly learning symbolic concepts like how graphical models do. However, a series of studies [Ren et al., 2021, 2023, Deng et al., 2022] have discovered that given a sufficiently-trained DNN for a classification task, its inference logic on a certain sample can usually be rewritten as the detection of specific concepts. In other words, the DNN’s inference score on a specific sample can be sparsely disentangled into effects of

a few concepts.

**Disentangling the DNN’s output as effects of interaction concepts.** Specifically, let us consider a trained DNN  $v : \mathbb{R}^n \rightarrow \mathbb{R}$  and an input sample  $\mathbf{x}$  with  $n$  input variables indexed by  $N = \{1, 2, \dots, n\}$ . Here, we assume the network output  $v(\mathbf{x}) \in \mathbb{R}$  is a scalar. Note that different settings can be applied to  $v(\mathbf{x})$ . For example, for multi-category classification tasks, we may set  $v(\mathbf{x}) = \log \frac{p(y=\mathbf{y}^{\text{true}}|\mathbf{x})}{1-p(y=\mathbf{y}^{\text{true}}|\mathbf{x})} \in \mathbb{R}$  by following [Deng et al., 2022]. Then, given a function  $v(\mathbf{x})$ , Ren et al. [2021] have proposed the following metric to quantify the interaction concept that is comprised of input variables in  $S \subseteq N$ .

$$I(S|\mathbf{x}) \triangleq \sum_{T \subseteq S} (-1)^{|S|-|T|} \cdot v(\mathbf{x}_T) \quad (1)$$

where  $\mathbf{x}_T$  denotes the input sample when we keep variables in  $T \subseteq N$  unchanged and mask variables in  $N \setminus T$  using baseline values<sup>1</sup>.

**Here, the interaction concept  $I(S|\mathbf{x})$  extracted from**

<sup>1</sup>For all tabular datasets and the image datasets (the *Celeba-eyeglasses* dataset and the *CUB-binary* dataset), the baseline value of each input variable was set as the mean value of this variable over all samples [Dabkowski and Gal, 2017]. For grayscale digital images in the *MNIST-3* dataset, the baseline value of each pixel was set as zero [Ancona et al., 2019]. For the point-cloud dataset, the baseline value was set as the center of the entire point cloud [Shen et al., 2021].

**the input  $\mathbf{x}$  encodes an AND relationship (interaction) between input variables in  $S$ .** For example, let us consider three image regions of  $S = \{\text{eyes, nose, mouth}\}$  that form the “face” concept in a face classification task. Then,  $I(S|\mathbf{x})$  measures the numerical effect of the concept on the classification score  $v(\mathbf{x})$ . Only when all image regions of “eyes”, “nose”, and “mouth” co-appear in the input image, the “face” concept is activated, and contributes a numerical effect  $I(S|\mathbf{x})$  to the classification score. Otherwise, if any region is masked, then the “face” concept cannot be formed, which removes the interaction effect, making  $I(S|\mathbf{x}_{\text{masked}}) = 0$ .

Mathematically, the above definition for an interaction concept can be understood as the Harsanyi dividend [Harsanyi, 1963] of  $S$  w.r.t. the DNN  $v$ . It has been proven that the DNN’s inference score  $v(\mathbf{x})$  can be disentangled into the sum of effects of all potential concepts, as follows.

$$v(\mathbf{x}) = \sum_{S \subseteq N} I(S|\mathbf{x}) \approx \sum_{S \in \Omega_{\mathbf{x}}} I(S|\mathbf{x}) \quad (2)$$

In particular, all interaction concepts can be further categorized into a set of **salient concepts**  $S \in \Omega_{\mathbf{x}}$  with considerable effects  $I(S|\mathbf{x})$ , and a set of ignorable **noisy patterns** with almost zero effects  $I(S|\mathbf{x}) \approx 0$ .

Note that the Harsanyi dividend  $I(S|\mathbf{x})$  also satisfies many desirable axioms/theorems, as introduced in Appendix A. The interaction effects can be further optimized using various tricks in [Ren et al., 2021] to pursue much more sparsity.

### 3.2. Visualization of interaction concepts

In this section, we visualize interaction concepts extracted from point-cloud data and tabular data. Note that a sample in the ShapeNet dataset [Yi et al., 2016] usually contains 2500 3D points. To simplify the visualization, we simply consider 8-10 semantic parts on the point cloud  $\mathbf{x}$ , which has been provided by the dataset.<sup>2</sup> Each semantic part is taken as a “single” input variable to the DNN. In this way, we visualize concepts consisting of semantic parts.

Fig. 1 shows interaction concepts  $S$  and the corresponding effects  $I(S|\mathbf{x})$  extracted by PointNet [Qi et al., 2017a] from different samples  $\mathbf{x}$  in the ShapeNet dataset. We find that the interaction concept  $S = \{\text{light, front wheel, mid frame}\}$  on five samples all makes positive effects  $I(S|\mathbf{x}) > 0$  to the PointNet’s output, whereas the interaction concept  $S = \{\text{handle, front wheel, front frame}\}$  usually makes negative effects  $I(S|\mathbf{x}) < 0$  to the PointNet’s output. Similarly, Fig. 2 shows interaction concepts extracted from two tabular datasets, i.e., the *wifi* dataset<sup>3</sup>, and the *tic-tac-toe* dataset<sup>3</sup>. We visualize interactions between different received signal

<sup>2</sup>For example, the ShapeNet dataset has provided the annotated parts for the *motorbike* category, including *gas tank, seat, handle, light, front wheel, back wheel, front frame, mid frame, and back frame*. Please see Appendix B.2 for details on the annotation of semantic parts.

*strength indicatons* (RSSIs) in the *wifi* dataset, and interactions between *board states* in the *tic-tac-toe* dataset. We also find that the same interaction concept usually makes similar effects to the network output on different input samples, which supports the conclusion in Section 3.3.2.

### 3.3. Does a DNN really learn symbolic concepts?

Although Ren et al. [2021] have claimed that the metric  $I(S|\mathbf{x})$  in Eq. (1) quantifies symbolic concepts encoded by a DNN, there is still no theory to guarantee a subset  $S \subseteq N$  with a salient effect  $I(S|\mathbf{x})$  faithfully represents a meaningful and transferable concept. Instead, we should not ignore the possibility that  $I(S|\mathbf{x})$  is just a mathematical transformation that ensures  $v(\mathbf{x}) = \sum_{S \subseteq N} I(S|\mathbf{x})$  in Eq. (2) on each specific sample. Therefore, in this study, we examine the counter-intuitive conjecture that a DNN learns symbolic concepts from the following four perspectives.

#### 3.3.1 Sparsity of the encoded concepts

According to Eq. (2), the DNN may encode at most  $2^n$  symbolic concepts in  $2^N \triangleq \{S : S \subseteq N\}$  w.r.t. the  $2^n$  different combinations of input variables. **However, a distinctive property of symbolism, which is different from connectionism, is that people usually would like to use a small number of explicit symbolic concepts to represent the knowledge, instead of using extensive fuzzy features.**

Thus, we hope to examine whether a DNN’s inference score  $v(\mathbf{x})$  on a specific sample can be summarized into effects of a small number of salient concepts  $v(\mathbf{x}) \approx \sum_{S \in \Omega_{\mathbf{x}}} I(S|\mathbf{x})$ , rather than using an exponential number of concepts w.r.t. all subsets  $S \subseteq N$ . To be precise, a faithful conceptual representation requires most concepts  $S \subseteq N$  to be noisy patterns with negligible effects  $I(S|\mathbf{x}) \approx 0$ . Only a few salient concepts  $S$  in  $\Omega_{\mathbf{x}}$  make considerable effects  $I(S|\mathbf{x})$ .

To this end, Ren et al. [2021] have made a preliminary attempt to explain a DNN’s inference score  $v(\mathbf{x})$  on a specific sample  $\mathbf{x}$  as interaction effects  $I(S|\mathbf{x})$  of a small number of concepts. Specifically, they used a few top-ranked salient interaction concepts to explain the inference score of LSTMs [Hochreiter and Schmidhuber, 1997] and CNNs [Kim, 2014] trained for sentiment classification and linguistic acceptance classification tasks on the SST-2 dataset [Socher et al., 2013] and the CoLA dataset [Warstadt et al., 2019].

**Experiments.** In this paper, we further examined whether most DNNs, which were trained for much more diverse tasks on different datasets, all encoded very sparse salient concepts. To this end, we trained various DNNs<sup>3</sup> on tabular datasets (the *tic-tac-toe* dataset<sup>3</sup> and the *wifi* dataset<sup>3</sup>), image datasets

<sup>3</sup>Please see the *experimental settings* paragraph at the end of Section 3 for details on datasets and DNNs.

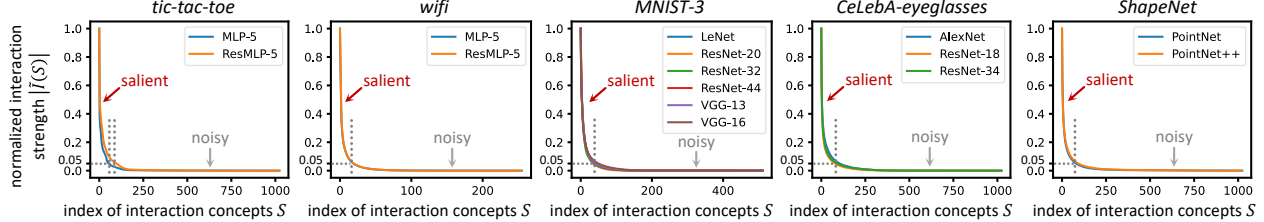


Figure 3. Normalized strength of interaction effects of different concepts in a descending order. DNNs trained for different tasks all encode sparse salient concepts.

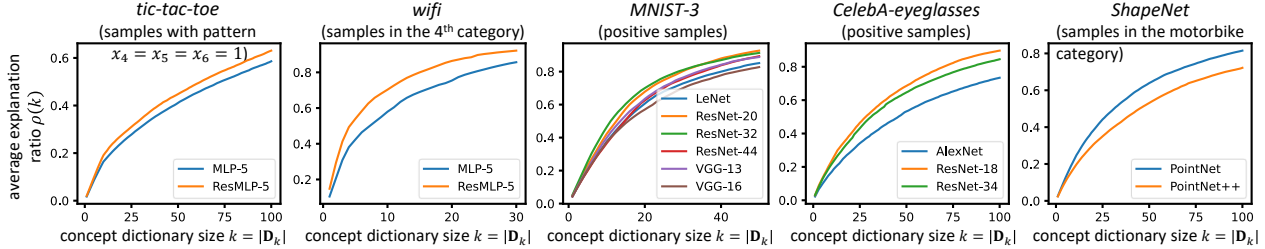


Figure 4. The change of the average explanation ratio  $\rho(k)$  along with the size  $k$  of the concept dictionary  $\mathbf{D}_k$ .

(the *MNIST-3* dataset<sup>3</sup> and the *CelebA-eyeglasses* dataset<sup>3</sup>), and a point-cloud dataset (the *ShapeNet* dataset<sup>3</sup>). The interaction effects can be further optimized using various tricks in [Ren et al., 2021] to pursue much more sparsity. Fig. 3 shows the normalized interaction strength of different concepts  $|\tilde{I}(S|\mathbf{x})| \triangleq |I(S|\mathbf{x})| / \max_{S'} |I(S'|\mathbf{x})|$  in a descending order for each DNN. Each curve shows the strength averaged over different samples in the dataset. We found that most concepts had little effects on the output  $|I(S|\mathbf{x})| \approx 0$ , which verified the sparsity of the encoded concepts.

**Salient concepts.** According to the above experiments, we can define the set of salient concepts as  $\Omega_{\mathbf{x}} = \{S : |I(S|\mathbf{x})| > \tau\}$ , subject to  $\tau = 0.05 \cdot \max_S |I(S|\mathbf{x})|$ . As Fig. 3 shows, there were only about 20-80 salient concepts extracted from an input sample, and all other concepts have ignorable effects on the network output.

### 3.3.2 Transferability over different samples

Beyond sparsity, the transferability of concepts is more important. If  $I(S|\mathbf{x})$  is just a tricky mathematical transformation on  $v(\mathbf{x}_S)$  without representing meaningful concepts, then each salient concept  $I(S|\mathbf{x})$  extracted from the input sample  $\mathbf{x}$  probably cannot be transferred to another input sample, *i.e.*, we cannot extract the same salient concept consisting of variables in  $S$  in the second sample, due to sparsity of salient concepts.

Therefore, in this section, we aim to verify whether concepts extracted from a sample can be transferred to other samples. This task is actually equivalent to checking whether there exists a common concept dictionary, which contains most salient concepts extracted from different samples in the same category.

Given a well-trained DNN, we construct a relatively small dictionary  $\mathbf{D}_k \subseteq 2^N$  containing the top- $k$  frequent concepts in different samples, and check whether such a dictionary contains most salient concepts in  $\Omega_{\mathbf{x}}$  extracted from each sample  $\mathbf{x}$ . The concept dictionary  $\mathbf{D}_k$  is constructed based on a greedy strategy. Specifically, we first extract a set of salient concepts  $\Omega_{\mathbf{x}}$  from each input sample  $\mathbf{x}$ . Then, we compute the frequency of each concept  $S$  being a salient concept over different samples. Finally, the concept dictionary  $\mathbf{D}_k$  is constructed to contain the top- $k$  interaction concepts with the highest frequencies.

Then, we design the metric  $\rho(k) \triangleq \mathbb{E}_{\mathbf{x}}[|\mathbf{D}_k \cap \Omega_{\mathbf{x}}| / |\Omega_{\mathbf{x}}|]$  to evaluate the average ratio of concepts extracted from an input sample that is covered by the concept dictionary  $\mathbf{D}_k$ . Theoretically, if we construct a larger dictionary  $\mathbf{D}_k$  with more concepts (a larger  $k$  value), then the dictionary can explain more concepts.

**Experiments.** We conducted experiments to show whether there existed a small concept dictionary that could explain most concepts encoded by the DNN. Specifically, we constructed a concept dictionary to explain samples in a certain category in each dataset<sup>4</sup>. In this experiment, we temporarily extracted salient concepts using  $\tau = 0.1 \cdot \max_S |I(S|\mathbf{x})|$  to construct  $\Omega_{\mathbf{x}}$ <sup>5</sup>. Fig. 4 shows the increase of the average explanation ratio  $\rho(k)$  along with the

<sup>4</sup>In this paper, when we needed to analyze of samples in a specific category, we used positive samples in the *MNIST-3*, *CelebA-eyeglasses*, and *CUB-binary* datasets, samples in the 4<sup>th</sup> category in the *wifi* dataset, and samples in the “motorbike” category in the *ShapeNet* dataset. For the *tic-tac-toe* dataset, since there exists eight sub-categories among positive samples, we used samples in the sub-category with the pattern  $x_4 = x_5 = x_6 = 1$ .

<sup>5</sup>Here, we increased the threshold from  $\tau = 0.05 \cdot \max_S |I(S|\mathbf{x})|$  to  $\tau = 0.1 \cdot \max_S |I(S|\mathbf{x})|$  to analyze those highly salient concepts. Appendix C.2 shows results computed by using the vanilla threshold  $\tau = 0.05 \cdot \max_S |I(S|\mathbf{x})|$  to compute  $\Omega_{\mathbf{x}}$ .

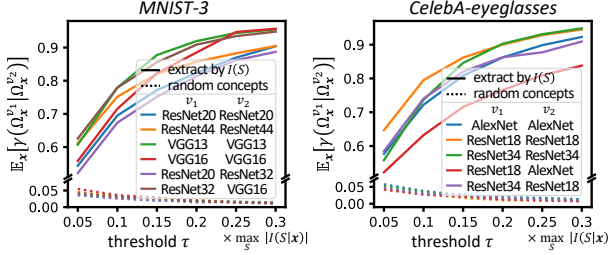


Figure 5. Concepts extracted by a higher threshold  $\tau$  (i.e. concepts with more significant effects  $I(S|\mathbf{x})$ ) usually have higher transferability across different DNNs.

increasing size  $k$  of the concept dictionary  $\mathbf{D}_k$ . We found that there usually existed a concept dictionary consisting of 30-100 concepts, which could explain more than 60%-80% salient concepts encoded by the DNN. Besides, Fig. 1(right) and Fig. 2(right) also show histograms of effects  $I(S|\mathbf{x})$  over different samples<sup>4</sup>, where  $S$  was extracted as a salient concept. We found that the same interaction concept usually made similar effects on different samples. This verified that the DNN learned transferable concepts over different samples.

### 3.3.3 Transferability across different DNNs

In addition to sample-wise transferability of concepts, another aspect is model-wise transferability. If the concepts extracted from an input sample really represent meaningful knowledge for the task, then these concepts are supposed to be stably learned by different DNNs towards the same task, although we cannot directly align intermediate-layer features between different DNNs.

Therefore, in this section, we aim to verify whether concepts extracted from a DNN can be transferred to another DNN trained for the same task. In other words, we actually check whether salient concepts encoded by one DNN are also encoded by another DNN learned for the same task. To this end, let us consider two DNNs,  $v_1$  and  $v_2$ , trained for the same task. Given an input sample  $\mathbf{x}$ , let  $\Omega_x^{v_1}$  and  $\Omega_x^{v_2}$  denote the sets of salient concepts extracted by  $v_1$  and  $v_2$  from the input sample  $\mathbf{x}$ , respectively. We evaluate the ratio of concepts in  $\Omega_x^{v_1}$  encoded by  $v_1$ , which are also encoded by  $v_2$  in  $\Omega_x^{v_2}$ , i.e.  $\gamma(\Omega_x^{v_1} | \Omega_x^{v_2}) \triangleq |\Omega_x^{v_1} \cap \Omega_x^{v_2}| / |\Omega_x^{v_1}|$ , to measure the transferability of salient concepts in  $\Omega_x^{v_1}$ . A larger ratio  $\gamma(\Omega_x^{v_1} | \Omega_x^{v_2})$  indicates that the extracted salient concepts have higher transferability across different DNNs.

**Experiments.** In this experiment, we examined the transferability of concepts in both the case when DNNs  $v_1$  and  $v_2$  had the same network architecture but were trained with different parameter initializations, and the case when  $v_1$  and  $v_2$  had different network architectures. Then, given each sample  $\mathbf{x}$ ,  $\Omega_x^{v_2}$  contains all salient concepts with interaction strength  $I_{v_2}(S|\mathbf{x}) \geq 0.05 \cdot \max_S |I_{v_2}(S|\mathbf{x})|$ , as defined in Sec-

tion 3.3.1. Whereas, we used different thresholds  $\tau$  ranging from  $\tau = 0.05 \cdot \max_S |I_{v_1}(S|\mathbf{x})|$  to  $\tau = 0.3 \cdot \max_S |I_{v_1}(S|\mathbf{x})|$  to generate different sets  $\Omega_x^{v_1}$ . A larger  $\tau$  value usually generated a smaller set of salient concepts with more significant effects. These concepts were more likely to be stably learned by different DNNs. Fig. 5 shows that concepts with higher saliency usually exhibited higher transferability from DNN  $v_1$  to DNN  $v_2$ . This indicated that more salient concepts were more likely to be stably learned by different DNNs, which was aligned with intuition. As a baseline for comparison, we also randomly extracted two sets of concepts  $\tilde{\Omega}_x^{v_1}$  and  $\tilde{\Omega}_x^{v_2}$  from all the  $2^n$  interaction concepts, which had the same size as  $\Omega_x^{v_1}$  and  $\Omega_x^{v_2}$ , i.e.  $|\Omega_x^{v_1}| = |\tilde{\Omega}_x^{v_1}|$  and  $|\Omega_x^{v_2}| = |\tilde{\Omega}_x^{v_2}|$ . Fig. 5 shows that the transferability  $\mathbb{E}_{\mathbf{x}}[\gamma(\Omega_x^{v_1} | \Omega_x^{v_2})]$  of concepts extracted by  $I(S|\mathbf{x})$  increased in the range of 0.5-0.95 along with the increase of  $\tau$ . In comparison, the transferability  $\mathbb{E}_{\mathbf{x}}[\gamma(\tilde{\Omega}_x^{v_1} | \tilde{\Omega}_x^{v_2})]$  of random concepts was usually less than 0.05. This verified the high transferability of concepts across different DNNs.

### 3.3.4 Discrimination power of concepts

Furthermore, if a DNN encodes faithful symbolic concepts, then these concepts are supposed to exhibit certain discrimination power in the classification task. In other words, **for each concept  $S$ , if the concept is saliently activated on a set of samples, then interaction effects  $I(S)$  of the same concept are supposed to push the classification of these samples towards a certain category in most cases.** Note that different concepts extracted from a sample may push the sample towards different categories, and the classification is the result of the competition between these concepts.

In order to verify the above discrimination power of concepts, in this section, we extract the concept  $S$  from  $m$  different input samples  $\mathbf{x}_1, \mathbf{x}_2, \dots, \mathbf{x}_m$  in the same category  $c$ , and check whether this concept consistently exhibits a positive (or negative) interaction effects  $I(S)$  on the  $m$  samples. If the concept  $S$  pushes the classification of most of the  $m$  samples towards the target category, i.e.,  $I(S|\mathbf{x}_i) > 0$  (or opposite to the target category, i.e.,  $I(S|\mathbf{x}_i) < 0$ ), then the discrimination power of the concept  $S$  is high. On the other hand, if the concept  $S$  pushes half of the samples towards the positive direction  $I(S|\mathbf{x}_i) > 0$ , but pushes the other half towards the negative direction  $I(S|\mathbf{x}_i) < 0$ , then the discrimination power of the concept  $S$  is low.

Specifically, we use the following metric to measure the discrimination power of concept  $S$  among the above  $m$  samples in category  $c$ . Let  $\Omega_{\mathbf{x}_i}$  denote a set of salient concepts extracted from the sample  $\mathbf{x}_i$ . Then,  $m_S^+ \triangleq \sum_i \mathbb{1}_{S \in \Omega_{\mathbf{x}_i}} \cdot \mathbb{1}_{I(S|\mathbf{x}_i) > 0}$  denote the number of samples where the concept  $S$  makes a salient and positive effect on the classification score. Similarly, we can define  $m_S^- \triangleq \sum_i \mathbb{1}_{S \in \Omega_{\mathbf{x}_i}} \cdot \mathbb{1}_{I(S|\mathbf{x}_i) < 0}$  to denote the number of samples where the concept  $S$  makes

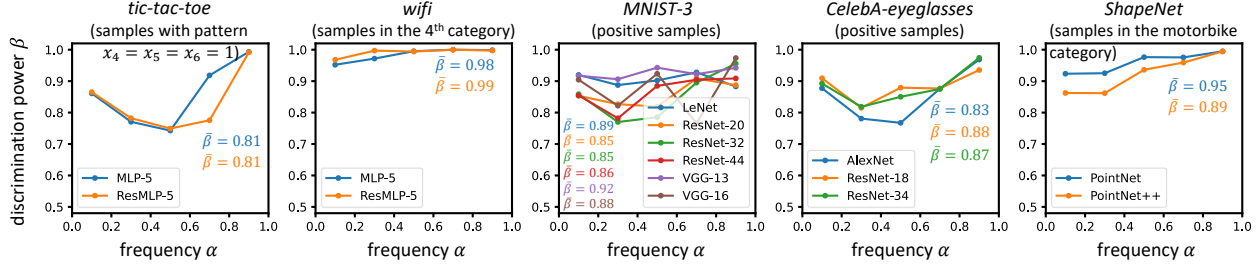


Figure 6. The average discrimination power of concepts in different frequency intervals, *i.e.*  $\alpha \in (0.0, 0.2], (0.2, 0.4], \dots, (0.8, 1.0]$ . The weighted average discrimination power  $\bar{\beta}$  over concepts of all frequencies is shown beside the curve.

a salient and negative effect on the classification score. In this way, the discrimination power of a salient concept  $S$  can be measured as  $\beta(S) = \max(m_S^+, m_S^-)/(m_S^+ + m_S^-)$ . A larger value of  $\beta(S)$  indicates a higher discrimination power of the concept  $S$ .

**Experiments.** Note that different concepts are of different importance in the classification of a category. Some concepts frequently appear in different samples and make salient effects, while other concepts only appear in very few concepts. Therefore, we use the frequency of the concept  $\alpha(S)$  as a weight to compute the average discrimination power of all concepts, which is given as  $\bar{\beta} \triangleq \sum_S [\alpha(S) \cdot \beta(S)] / \sum_S [\alpha(S)]$ . The frequency of a concept is defined as  $\alpha(S) \triangleq (m_S^+ + m_S^-)/m$ . The selection of datasets and the training of DNNs are introduced in the *experimental settings* paragraph at the end of Section 3. Fig. 6 shows the average discrimination power of concepts in different frequency intervals. We found that the average discrimination power  $\bar{\beta}$  of concepts was usually higher than 0.8, which verified the discrimination power of extracted concepts.

### 3.4. When DNNs do not learn transferable concepts

It is worth noting that all the above work just conducts experiments to show the concept-emerging phenomenon in different DNNs for different tasks. We do not provide, or there may even do not exist, a theoretical proof for such a concept-emerging phenomenon, although the concept-emerging phenomenon **does exist** in DNNs for most applications. Therefore, in this subsection, we would like to discuss the following three extreme cases, in which a DNN does not learn symbolic concepts.

In the three extreme cases, DNNs may either collapse to simple models close to linear regressions, or learn non-transferable indiscriminative concepts, although the network output can still be represented as the sum of interaction effects of these concepts.

• **Case 1: When there exists label noise.** If the ground-truth label for classification is incorrectly annotated on some samples, then the DNN usually has to memorize each incorrectly-labeled training sample for classification without summarizing many common features from such chaotic an-

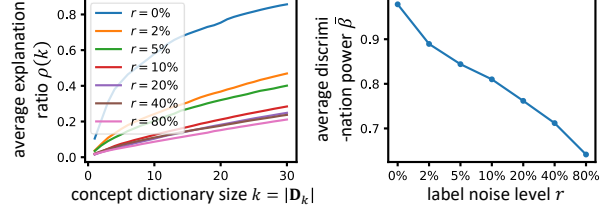


Figure 7. The (left) transferability and (right) discrimination power of concepts decreased when we added more label noises.

notations. Thus, in this case, the DNN usually encodes more non-transferable concepts.

**Experimental verification.** In this experiment, we constructed datasets with noisy labels to check whether DNNs trained on these datasets did not learn transferable concepts with high discrimination power. To this end, given a clean dataset, we first selected and randomly labeled a certain portion  $r$  of training samples in the dataset, so as to train a DNN. Specifically, we constructed a series of datasets by assigning different ratios  $r$  of samples with incorrect labels. We used the *wifi* dataset<sup>3</sup> to construct new datasets by adding different ratios  $r$  of noisy labels. Then, we trained an MLP-5 network<sup>3</sup> on each of these datasets. We examined the transferability and discrimination power of the extracted concepts<sup>4</sup> on each MLP-5 network. We extracted concept dictionaries of different sizes based on each MLP-5 network (please see Section 3.3.2 for details). Fig. 7(left) shows that if there was significant label noise in the dataset, the concept dictionary usually explained much fewer concepts encoded by the network, which indicated low transferability of the learned concepts. Besides, Fig. 7(right) shows the average discrimination power  $\bar{\beta}$  of the extracted concepts also decreased when we assigned more training samples with random labels. This verified that the DNN usually could not learn transferable and discriminative concepts from samples that were incorrectly labeled.

• **Case 2: When input samples are noisy.** In fact, this case can be extended to a more general scenario, *i.e.*, when the task is difficult to learn, there is no essential difference between the difficult data and noisy data for the DNN. Specifically, when training samples are noisy and lack meaningful

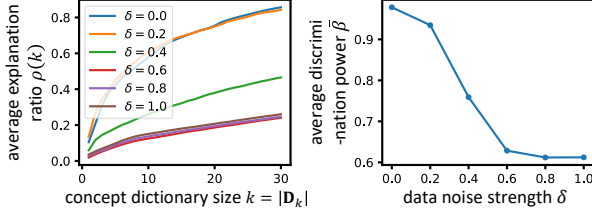


Figure 8. The (left) transferability and (right) discrimination power of concepts decreased when input data were noisy.

patterns, it is difficult for a DNN to learn transferable concepts from noisy training samples.

**Experimental verification.** In this experiment, we injected noise into training samples to examine whether DNNs trained on datasets with noisy samples did not learn transferable concepts. Just like the experiment in ‘‘Case 1,’’ we constructed such datasets by corrupting a clean dataset. To this end, we added Gaussian noises  $\epsilon \sim \mathcal{N}(\mathbf{0}, \mathbf{I})$  to each input sample  $\mathbf{x}$  in the clean dataset by modifying it to  $(1-\delta) \cdot \mathbf{x} + \delta \cdot \epsilon$ , where  $\delta \in [0, 1]$  denotes the strength of noise injected into the sample  $\mathbf{x}$ . Each dimension of the clean sample  $\mathbf{x}$  was normalized to unit variance over the dataset beforehand.

We constructed a series of datasets by injecting noises of different strength  $\delta$  into samples in the *wifi* dataset<sup>3</sup>. We trained MLP-5’s<sup>3</sup> based on these datasets. Just like experiments in ‘‘Case 1,’’ we examined the transferability and discrimination power of concepts. Fig. 8(left) shows that the transferability of concepts was usually low when the DNN was learned from noisy input data. Fig. 8(right) shows that the average discrimination power  $\bar{\beta}$  of concepts decreased along with the increasing strength  $\delta$  of injected noise. This verified that DNN usually did not learn transferable and discriminative concepts when input data were noisy.

• **Case 3: When the task has a simple shortcut solution.** In the above two cases, both label noise and data noise corrupted the original discriminative patterns in each category, thus making the DNN unlikely to learn transferable concepts. In comparison, here, let us discuss a new case, *i.e.*, even if there exist meaningful patterns in training data, the DNN may still not learn these concepts.

To be precise, if a classification task can be conducted with some shortcut solutions without requiring the DNN to encode complex concepts, then the DNN probably converges to the shortcut solution. For example, in an image classification task, if pixel-wise colors are sufficient to conduct the image-classification task, then the DNN is more likely to only use the color information for classification without modeling complex visual concepts. The simple shortcut solution usually prevents the DNN from summarizing complex visual concepts.

**Experimental verification.** We constructed a dataset for image classification, where the ‘‘color’’ information was a shortcut solution for the task. Specifically, we modified

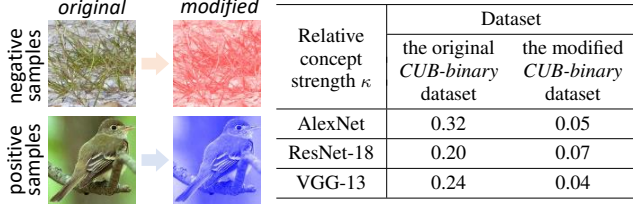


Figure 9. (left) We constructed a dataset where the ‘‘color’’ information was a shortcut solution. (right) The relative concept strength  $\kappa$  extracted from DNNs trained on different datasets.

images in the *CUB-binary* dataset<sup>3</sup>, such that all negative samples were red-colored background regions, and all positive samples were blue-colored foreground birds, as shown in Fig. 9(left). We trained AlexNet, ResNet-18, and VGG-13 on both the original dataset and the modified dataset. Compared with DNNs learned on the original dataset, DNNs learned on the modified dataset were more likely to simply use the color information for classification. We used the metric  $\kappa \triangleq \mathbb{E}_{\mathbf{x}}[\sum_{S \in \Omega_{\mathbf{x}}, |S| \geq 2} |I(S)| / \sum_{S \in \Omega_{\mathbf{x}}} |I(S)|]$  to measure the relative strength of all concepts consisting of multiple variables. Fig. 9(right) shows that the  $\kappa$  values were usually low for DNNs learned to classify red-colored backgrounds and blue-colored birds. This indicated that the DNN collapsed to a simple model without encoding interactions between different image patches when the task had a simple shortcut solution.

**Experimental settings.** For tabular datasets, we used the UCI tic-tac-toe endgame dataset [Dua and Graff, 2017] for binary classification, and used the UCI wireless indoor localization dataset [Dua and Graff, 2017] for multi-category classification. These datasets were termed *tic-tac-toe* and *wifi* for simplicity. We trained the following two MLPs on each tabular dataset. *MLP-5* contained five fully connected layers with 100 neurons in each hidden layer [Ren et al., 2021]. *ResMLP-5* was constructed by adding a skip connection to each layer of an *MLP-5*. For image data, we used the following three datasets. We took images corresponding to digit ‘‘three’’ in the MNIST dataset [LeCun, 1998] as positive samples, and took other images as negative samples to train DNNs. We took images with the attribute ‘‘eyeglasses’’ in the CelebA dataset [Liu et al., 2015] as positive samples, and took other images as negative samples to train DNNs. We trained DNNs to classify birds in bounding boxes in the CUB-200-2011 dataset [Wah et al., 2011] from randomly cropped background regions around the bird. These three datasets were termed *MNIST-3*, *CelebA-eyeglasses*, and *CUB-binary* for short. We trained LeNet [LeCun et al., 1998], AlexNet [Krizhevsky et al., 2017], ResNet-18/20/32/34/44 [He et al., 2016], VGG-13/16 [Simonyan and Zisserman, 2014] on these image datasets. Based on the ShapeNet dataset [Yi et al., 2016] for the classification of 3D point clouds, we trained PointNet [Qi et al., 2017a] and

PointNet++ [Qi et al., 2017b]. Please see Appendix B.1 for the classification accuracy of the above DNNs.

## 4. Conclusion

In this paper, we have analyzed the interaction concepts encoded by a DNN. Specifically, we quantitatively examine the concept-emerging phenomenon of a DNN from four perspectives. Extensive empirical studies have verified that a well-trained DNN usually encodes sparse, transferable, and discriminative interaction concepts. Our experiments also prove the faithfulness of the interaction concepts extracted from DNNs. Besides, we also discussed three cases in which a DNN is unlikely to learn transferable concepts.

## References

Marco Ancona, Cengiz Oztireli, and Markus Gross. Explaining deep neural networks with a polynomial time algorithm for shapley value approximation. In *International Conference on Machine Learning*, pages 272–281. PMLR, 2019.

David Bau, Bolei Zhou, Aditya Khosla, Aude Oliva, and Antonio Torralba. Network dissection: Quantifying interpretability of deep visual representations. In *Proceedings of the IEEE conference on computer vision and pattern recognition*, pages 6541–6549, 2017.

Zhengping Che, Sanjay Purushotham, Robinder Khemani, and Yan Liu. Interpretable deep models for icu outcome prediction. In *AMIA annual symposium proceedings*, volume 2016, page 371. American Medical Informatics Association, 2016.

Ian Covert, Scott M Lundberg, and Su-In Lee. Understanding global feature contributions with additive importance measures. *Advances in Neural Information Processing Systems*, 33, 2020.

Piotr Dabkowski and Yarin Gal. Real time image saliency for black box classifiers. *arXiv preprint arXiv:1705.07857*, 2017.

Huiqi Deng, Qihan Ren, Hao Zhang, and Quanshi Zhang. Discovering and explaining the representation bottleneck of dnns. In *International Conference on Learning Representations*, 2022.

Alexey Dosovitskiy and Thomas Brox. Inverting visual representations with convolutional networks. In *Proceedings of the IEEE Conference on Computer Vision and Pattern Recognition*, pages 4829–4837, 2016.

Dheeru Dua and Casey Graff. UCI machine learning repository, 2017. URL <http://archive.ics.uci.edu/ml>.

Ruth C Fong and Andrea Vedaldi. Interpretable explanations of black boxes by meaningful perturbation. In *Proceedings of the IEEE international conference on computer vision*, pages 3429–3437, 2017.

Nicholas Frosst and Geoffrey Hinton. Distilling a neural network into a soft decision tree. *arXiv preprint arXiv:1711.09784*, 2017.

Michel Grabisch and Marc Roubens. An axiomatic approach to the concept of interaction among players in cooperative games. *International Journal of game theory*, 28(4):547–565, 1999.

John C Harsanyi. A simplified bargaining model for the n-person cooperative game. *International Economic Review*, 4(2):194–220, 1963.

Kaiming He, Xiangyu Zhang, Shaoqing Ren, and Jian Sun. Deep residual learning for image recognition. In *Proceedings of the IEEE conference on computer vision and pattern recognition*, pages 770–778, 2016.

Sepp Hochreiter and Jürgen Schmidhuber. Long short-term memory. *Neural computation*, 9(8):1735–1780, 1997.

Joseph D Janizek, Pascal Sturmfels, and Su-In Lee. Explaining explanations: Axiomatic feature interactions for deep networks. *arXiv preprint arXiv:2002.04138*, 2020.

Xisen Jin, Zhongyu Wei, Junyi Du, Xiangyang Xue, and Xiang Ren. Towards hierarchical importance attribution: Explaining compositional semantics for neural sequence models. In *International Conference on Learning Representations*, 2019.

Been Kim, Martin Wattenberg, Justin Gilmer, Carrie Cai, James Wexler, Fernanda Viegas, et al. Interpretability beyond feature attribution: Quantitative testing with concept activation vectors (tcav). In *International conference on machine learning*, pages 2668–2677. PMLR, 2018.

Yoon Kim. Convolutional neural networks for sentence classification. In *Proceedings of the 2014 Conference on Empirical Methods in Natural Language Processing (EMNLP)*, pages 1746–1751, Doha, Qatar, October 2014. Association for Computational Linguistics. doi: 10.3115/v1/D14-1181. URL <https://aclanthology.org/D14-1181>.

Alex Krizhevsky, Ilya Sutskever, and Geoffrey E Hinton. Imagenet classification with deep convolutional neural networks. *Communications of the ACM*, 60(6):84–90, 2017.

Yann LeCun. The mnist database of handwritten digits. <http://yann.lecun.com/exdb/mnist/>, 1998.

Yann LeCun, Léon Bottou, Yoshua Bengio, and Patrick Haffner. Gradient-based learning applied to document recognition. *Proceedings of the IEEE*, 86(11):2278–2324, 1998.

Ziwei Liu, Ping Luo, Xiaogang Wang, and Xiaoou Tang. Deep learning face attributes in the wild. In *Proceedings of International Conference on Computer Vision (ICCV)*, December 2015.

Scott M Lundberg and Su-In Lee. A unified approach to interpreting model predictions. In I. Guyon, U. V. Luxburg, S. Bengio, H. Wallach, R. Fergus, S. Vishwanathan, and R. Garnett, editors, *Advances in Neural Information Processing Systems*, volume 30. Curran Associates, Inc., 2017a. URL <https://proceedings.neurips.cc/paper/2017/file/8a20a8621978632d76c43dfd28b67767-Paper.pdf>.

Scott M Lundberg and Su-In Lee. A unified approach to interpreting model predictions. In *Proceedings of the 31st international conference on neural information processing systems*, pages 4768–4777, 2017b.

W James Murdoch, Peter J Liu, and Bin Yu. Beyond word importance: Contextual decomposition to extract interactions from lstms. In *International Conference on Learning Representations*, 2018.

Charles R Qi, Hao Su, Kaichun Mo, and Leonidas J Guibas. Pointnet: Deep learning on point sets for 3d classification and segmentation. In *Proceedings of the IEEE conference on computer vision and pattern recognition*, pages 652–660, 2017a.

Charles Ruizhongtai Qi, Li Yi, Hao Su, and Leonidas J Guibas. Pointnet++: Deep hierarchical feature learning on point sets in a metric space. *Advances in neural information processing systems*, 30, 2017b.

Jie Ren, Mingjie Li, Qihan Ren, Huiqi Deng, and Quanshi Zhang. Towards axiomatic, hierarchical, and symbolic explanation for deep models. *arXiv preprint arXiv:2111.06206*, 2021.

Jie Ren, Zhanpeng Zhou, Qirui Chen, and Quanshi Zhang. Can we faithfully represent absence states to compute Shapley values on a DNN? In *International Conference on Learning Representations*, 2023. URL <https://openreview.net/forum?id=YV8tP7bW6Kt>.

Marco Tulio Ribeiro, Sameer Singh, and Carlos Guestrin. " why should i trust you?" explaining the predictions of any classifier. In *Proceedings of the 22nd ACM SIGKDD international conference on knowledge discovery and data mining*, pages 1135–1144, 2016.

Ramprasaath R Selvaraju, Michael Cogswell, Abhishek Das, RamaKrishna Vedantam, Devi Parikh, and Dhruv Batra. Grad-cam: Visual explanations from deep networks via gradient-based localization. In *Proceedings of the IEEE international conference on computer vision*, pages 618–626, 2017.

Lloyd S Shapley. A value for n-person games. *Contributions to the Theory of Games*, 2(28):307–317, 1953.

Wen Shen, Qihan Ren, Dongrui Liu, and Quanshi Zhang. Interpreting representation quality of dnns for 3d point cloud processing. *Advances in Neural Information Processing Systems*, 34:8857–8870, 2021.

Karen Simonyan and Andrew Zisserman. Very deep convolutional networks for large-scale image recognition. *arXiv preprint arXiv:1409.1556*, 2014.

Karen Simonyan, Andrea Vedaldi, and Andrew Zisserman. Deep inside convolutional networks: Visualising image classification models and saliency maps. *arXiv preprint arXiv:1312.6034*, 2013.

Chandan Singh, W James Murdoch, and Bin Yu. Hierarchical interpretations for neural network predictions. In *International Conference on Learning Representations*, 2018.

Richard Socher, Alex Perelygin, Jean Wu, Jason Chuang, Christopher D Manning, Andrew Y Ng, and Christopher Potts. Recursive deep models for semantic compositionality over a sentiment treebank. In *Proceedings of the 2013 conference on empirical methods in natural language processing*, pages 1631–1642, 2013.

Daria Sorokina, Rich Caruana, Mirek Riedewald, and Daniel Fink. Detecting statistical interactions with additive groves of trees. In *Proceedings of the 25th international conference on Machine learning*, pages 1000–1007, 2008.

Mukund Sundararajan, Ankur Taly, and Qiqi Yan. Axiomatic attribution for deep networks. In *International conference on machine learning*, pages 3319–3328. PMLR, 2017.

Mukund Sundararajan, Kedar Dhamdhere, and Ashish Agarwal. The shapley taylor interaction index. In *International Conference on Machine Learning*, pages 9259–9268. PMLR, 2020.

Sarah Tan, Rich Caruana, Giles Hooker, Paul Koch, and Albert Gordo. Learning global additive explanations for neural nets using model distillation. *arXiv preprint arXiv:1801.08640*, 2018.

Che-Ping Tsai, Chih-Kuan Yeh, and Pradeep Ravikumar. Faithshap: The faithful shapley interaction index. *arXiv preprint arXiv:2203.00870*, 2022.

Joel Vaughan, Agus Sudjianto, Erind Brahimi, Jie Chen, and Vijayan N Nair. Explainable neural networks based on additive index models. *arXiv preprint arXiv:1806.01933*, 2018.

Catherine Wah, Steve Branson, Peter Welinder, Pietro Perona, and Serge Belongie. The caltech-ucsd birds-200-2011 dataset. , 2011.

Alex Warstadt, Amanpreet Singh, and Samuel R Bowman. Neural network acceptability judgments. *Transactions of the Association for Computational Linguistics*, 7:625–641, 2019.

Mike Wu, Michael C Hughes, Sonali Parbhoo, Maurizio Zazzi, Volker Roth, and Finale Doshi-Velez. Beyond sparsity: Tree regularization of deep models for interpretability. In *Thirty-Second AAAI Conference on Artificial Intelligence*, 2018.

Li Yi, Vladimir G Kim, Duygu Ceylan, I-Chao Shen, Mengyan Yan, Hao Su, Cewu Lu, Qixing Huang, Alla Sheffer, and Leonidas Guibas. A scalable active framework for region annotation in 3d shape collections. *ACM Transactions on Graphics (ToG)*, 35(6):1–12, 2016.

Jason Yosinski, Jeff Clune, Anh Nguyen, Thomas Fuchs, and Hod Lipson. Understanding neural networks through deep visualization. In *International Conference on Machine Learning*, 2015.

Matthew D Zeiler and Rob Fergus. Visualizing and understanding convolutional networks. In *European conference on computer vision*, pages 818–833. Springer, 2014.

Quanshi Zhang, Ruiming Cao, Feng Shi, Ying Nian Wu, and Song-Chun Zhu. Interpreting cnn knowledge via an explanatory graph. In *Thirty-Second AAAI Conference on Artificial Intelligence*, 2018.

Bolei Zhou, Aditya Khosla, Agata Lapedriza, Aude Oliva, and Antonio Torralba. Object detectors emerge in deep scene cnns. *In ICLR*, 2015.

Bolei Zhou, Aditya Khosla, Agata Lapedriza, Aude Oliva, and Antonio Torralba. Learning deep features for discriminative localization. In *Proceedings of the IEEE conference on computer vision and pattern recognition*, pages 2921–2929, 2016.

## A. Axioms and theorems of the Harsanyi dividend

As mentioned in Section 3.1 of the paper, the definition for an interaction concept  $S$  in Eq. (1) can be understood as the Harsanyi dividend of the set of variables in  $S$  w.r.t. the DNN  $v$ . In fact, the Harsanyi dividend  $I(S|\mathbf{x})$  also satisfies many desirable axioms and theorems, as follows.

The Harsanyi dividend  $I(S|\mathbf{x})$  satisfies seven desirable axioms in game theory Ren et al. [2021], including the *efficiency*, *linearity*, *dummy*, *symmetry*, *anonymity*, *recursive* and *interaction distribution* axioms.

(1) *Efficiency axiom*. The output score of a model can be decomposed into interaction effects of different patterns, *i.e.*  $v(\mathbf{x}) = \sum_{S \subseteq N} I(S|\mathbf{x})$ .

(2) *Linearity axiom*. If we merge output scores of two models  $w$  and  $v$  as the output of model  $u$ , *i.e.*  $\forall S \subseteq N, u(\mathbf{x}_S) = w(\mathbf{x}_S) + v(\mathbf{x}_S)$ , then their interaction effects  $I_v(S|\mathbf{x})$  and  $I_w(S|\mathbf{x})$  can also be merged as  $\forall S \subseteq N, I_u(S|\mathbf{x}) = I_v(S|\mathbf{x}) + I_w(S|\mathbf{x})$ .

(3) *Dummy axiom*. If a variable  $i \in N$  is a dummy variable, *i.e.*  $\forall S \subseteq N \setminus \{i\}, v(\mathbf{x}_{S \cup \{i\}}) = v(\mathbf{x}_S) + v(\mathbf{x}_{\{i\}})$ , then it has no interaction with other variables,  $\forall \emptyset \neq T \subseteq N \setminus \{i\}, I(T \cup \{i\}|\mathbf{x}) = 0$ .

(4) *Symmetry axiom*. If input variables  $i, j \in N$  cooperate with other variables in the same way,  $\forall S \subseteq N \setminus \{i, j\}, v(\mathbf{x}_{S \cup \{i\}}) = v(\mathbf{x}_{S \cup \{j\}})$ , then they have same interaction effects with other variables,  $\forall S \subseteq N \setminus \{i, j\}, I(S \cup \{i\}|\mathbf{x}) = I(S \cup \{j\}|\mathbf{x})$ .

(5) *Anonymity axiom*. For any permutations  $\pi$  on  $N$ , we have  $\forall S \subseteq N, I_v(S|\mathbf{x}) = I_{\pi v}(\pi S|\mathbf{x})$ , where  $\pi S \triangleq \{\pi(i) | i \in S\}$ , and the new model  $\pi v$  is defined by  $(\pi v)(\mathbf{x}_{\pi S}) = v(\mathbf{x}_S)$ . This indicates that interaction effects are not changed by permutation.

(6) *Recursive axiom*. The interaction effects can be computed recursively. For  $i \in N$  and  $S \subseteq N \setminus \{i\}$ , the interaction effect of the pattern  $S \cup \{i\}$  is equal to the interaction effect of  $S$  with the presence of  $i$  minus the interaction effect of  $S$  with the absence of  $i$ , *i.e.*  $\forall S \subseteq N \setminus \{i\}, I(S \cup \{i\}|\mathbf{x}) = I(S|i \text{ is always present, } \mathbf{x}) - I(S|\mathbf{x})$ .  $I(S|i \text{ is always present, } \mathbf{x})$  denotes the interaction effect when the variable  $i$  is always present as a constant context, *i.e.*  $I(S|i \text{ is always present, } \mathbf{x}) = \sum_{L \subseteq S} (-1)^{|S|-|L|} \cdot v(\mathbf{x}_{L \cup \{i\}})$ .

(7) *Interaction distribution axiom*. This axiom characterizes how interactions are distributed for “interaction functions” Sundararajan et al. [2020]. An interaction function  $v_T$  parameterized by a subset of variables  $T$  is defined as follows.  $\forall S \subseteq N$ , if  $T \subseteq S, v_T(\mathbf{x}_S) = c$ ; otherwise,  $v_T(\mathbf{x}_S) = 0$ . The function  $v_T$  models pure interaction among the variables in  $T$ , because only if all variables in  $T$  are present, the output value will be increased by  $c$ . The interactions encoded in the function  $v_T$  satisfies  $I(T|\mathbf{x}) = c$ , and  $\forall S \neq T, I(S|\mathbf{x}) = 0$ .

The Harsanyi dividend  $I(S|\mathbf{x})$  can also explain the elementary mechanism of existing game-theoretic metrics Ren et al. [2021], including the *Shapley value*, the *Shapley interaction index*, and the *Shapley-Taylor interaction index*.

(1) *Connection to the Shapley value* Shapley [1953]. Let  $\phi(i|\mathbf{x})$  denote the Shapley value of an input variable  $i$ , given the input sample  $\mathbf{x}$ . Then, the Shapley value  $\phi(i|\mathbf{x})$  can be explained as the result of uniformly assigning attributions of each Harsanyi dividend to each involving variable  $i$ , *i.e.*,  $\phi(i|\mathbf{x}) = \sum_{S \subseteq N \setminus \{i\}} \frac{1}{|S|+1} I(S \cup \{i\}|\mathbf{x})$ . This also proves that the Shapley value is a fair assignment of attributions from the perspective of Harsanyi dividend.

(2) *Connection to the Shapley interaction index* Grabisch and Roubens [1999]. Given a subset of variables  $T \subseteq N$  in an input sample  $\mathbf{x}$ , the Shapley interaction index  $I^{\text{Shapley}}(T|\mathbf{x})$  can be represented as  $I^{\text{Shapley}}(T|\mathbf{x}) = \sum_{S \subseteq N \setminus T} \frac{1}{|S|+1} I(S \cup T|\mathbf{x})$ . In other words, the index  $I^{\text{Shapley}}(T|\mathbf{x})$  can be explained as uniformly allocating  $I(S'|\mathbf{x})$  s.t.  $S' = S \cup T$  to the compositional variables of  $S'$ , if we treat the coalition of variables in  $T$  as a single variable.

(3) *Connection to the Shapley Taylor interaction index* Sundararajan et al. [2020]. Given a subset of variables  $T \subseteq N$  in an input sample  $\mathbf{x}$ , the  $k$ -th order Shapley Taylor interaction index  $I^{\text{Shapley-Taylor}}(T|\mathbf{x})$  can be represented as weighted sum of interaction effects, *i.e.*,  $I^{\text{Shapley-Taylor}}(T|\mathbf{x}) = I(T|\mathbf{x})$  if  $|T| < k$ ;  $I^{\text{Shapley-Taylor}}(T|\mathbf{x}) = \sum_{S \subseteq N \setminus T} \binom{|S|+k}{k}^{-1} I(S \cup T|\mathbf{x})$  if  $|T| = k$ ; and  $I^{\text{Shapley-Taylor}}(T|\mathbf{x}) = 0$  if  $|T| > k$ .

## B. Experimental details

### B.1. Accuracy of DNNs

In this paper, we conducted experiments on various DNNs trained on different types of datasets, including tabular datasets, image datasets, and a point-cloud dataset. Table 1 reports the classification accuracy of DNNs trained on the above datasets.

### B.2. The annotation of semantic parts

This section discusses the annotation of semantic parts in the point-cloud dataset and image datasets. As mentioned in Section 3.3.1, given an input sample  $\mathbf{x}$  with  $n$  input variables, the DNN may encode at most  $2^n$  interaction concepts. The computational cost for extracting salient concepts is high, when the number of input variables  $n$  is large. For example, if we take each 3D point of a point-cloud (or each pixel of an image) as a single input variable, the computation is usually prohibitive. In order to overcome this issue, we simply annotate 8-10 semantic parts in each input sample, such that the annotated semantic

Table 1. Classification accuracy of different DNNs.

Dataset	DNN					
<i>tic-tac-toe</i>	MLP-5 100%	ResMLP-5 100%				
<i>wifi</i>	MLP-5 97.75%	ResMLP-5 97.75%				
<i>MNIST-3</i>	LeNet 99.99%	ResNet-20 100%	ResNet-32 100%	ResNet-44 100%	VGG-13 100%	VGG-16 100%
<i>CelebA-eyeglasses</i>	AlexNet 99.53%	ResNet-18 99.66%	VGG-13 99.65%			
<i>CUB-binary</i>	AlexNet 95.67%	ResNet-18 96.41%	ResNet-34 96.43%			
the modified <i>CUB-binary</i> dataset	AlexNet 100%	ResNet-18 100%	ResNet-34 100%			
<i>ShapeNet</i>	PointNet 97.36%	PointNet++ 98.64%				

parts are aligned over different samples. Then, each semantic part in an input sample is taken as a “single” input variable to the DNN.

- For point-cloud data in the ShapeNet dataset, we annotated semantic parts for 100 samples in the *motorbike* category. These semantic parts were generated based on original annotations provided by Yi et al. [2016]. In the original annotation, Yi et al. [2016] provided semantic parts including *gas tank*, *seat*, *handle*, *light*, *wheel*, and *frame* for each *motorbike* sample. As shown in Fig. 10, we further modified the original annotation into more fine-grained semantic parts, *i.e.* *gas tank*, *seat*, *handle*, *light*, *front wheel*, *back wheel*, *front frame*, *mid frame*, and *back frame*.

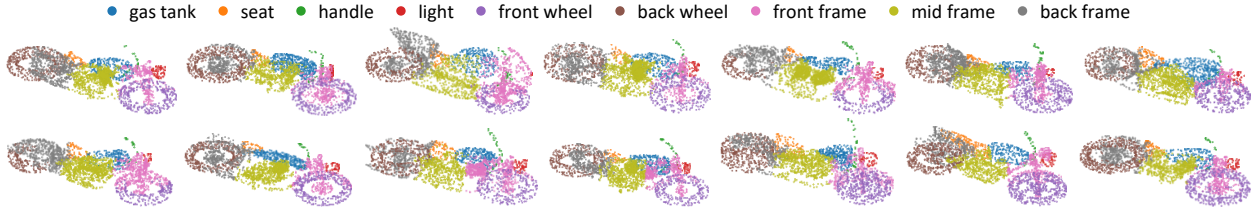


Figure 10. Examples of annotated semantic parts for samples in the *motorbike* category of the ShapeNet dataset.

- For image data, we annotated semantic parts for 50 samples in the *CelebA-eyeglasses* dataset and 20 samples in the *CUB-binary* dataset. Specifically, as shown in Fig. 11, we annotated semantic parts including *forehead*, *left eye*, *right eye*, *nose*, *left cheek*, *right cheek*, *mouth*, *chin*, and *hair* for each sample in the *CelebA-eyeglasses* dataset<sup>6</sup>. As shown in Fig. 12, we annotated semantic parts including *head*, *neck*, *throat*, *wing*, *tail*, *leg*, *belly*, and *breast* for each sample in the *CUB-binary* dataset<sup>6</sup>.

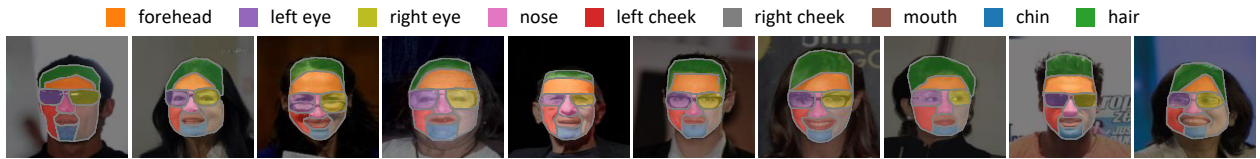


Figure 11. Examples of annotated semantic parts for positive samples in the *CelebA-eyeglasses* dataset.

- For images in the *MNIST-3* dataset, we annotated semantic parts for 100 positive samples. For each single image in this dataset, most pixels were black background pixels, which had no interaction effects with pixels in the foreground. Therefore, we similarly considered interactions only within foreground pixels. Besides, since there usually did not exist semantic parts with clear meanings in hand-written digit images, we annotated different parts based on some keypoints in each image. As shown in Fig. 13, we annotate eight parts based on eight keypoints in each image<sup>6</sup>.

<sup>6</sup>Note that we only considered interactions within foreground regions in each image, due to the high computational cost mentioned above. Therefore, the annotated semantic parts did not cover regions in the background. Please see Section B.4 for details on how to handle background regions in the computation of  $I(S|\mathbf{x})$  for image data.



Figure 12. Examples of annotated semantic parts for positive samples in the *CUB-binary* dataset.

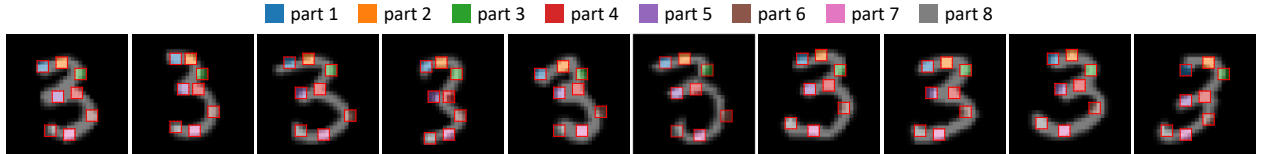


Figure 13. Examples of annotated semantic parts for positive samples in the *MNIST-3* dataset.

### B.3. The setting of $v(\mathbf{x})$ in experiments

As mentioned in Section 3.1 of the paper, in the computation of the interaction effect  $I(S|\mathbf{x})$ , people can apply different settings for  $v(\mathbf{x})$ . For example, Covert et al. [2020] computed  $v(\mathbf{x})$  as the cross-entropy loss of the sample  $\mathbf{x}$  in the classification task. Lundberg and Lee [2017b] directly set  $v(\mathbf{x}) = p(y = y^{\text{truth}}|\mathbf{x}) \in \mathbb{R}$ . In this paper, we followed Deng et al. [2022] and used  $v(\mathbf{x}) = \log \frac{p(y = y^{\text{truth}}|\mathbf{x})}{1 - p(y = y^{\text{truth}}|\mathbf{x})} \in \mathbb{R}$  for both binary classification tasks and multi-category classification tasks.

### B.4. Computation details of $I(S|\mathbf{x})$ for image data

As mentioned in Section B.2, given an input sample  $\mathbf{x}$  with  $n$  input variables, the DNN may encode at most  $2^n$  interaction concepts. The computational cost for extracting salient concepts is high, when the number of input variables  $n$  is large. In order to overcome this issue, we only considered interaction concepts formed by foreground regions. For image data, the annotated semantic parts for each sample only covered regions in the foreground. In order to handle the uncovered regions in the background, in the extraction of interaction concepts, we averaged the interaction effect  $I(S|\mathbf{x})$  when we were given multiple background with different strengths, which was similar to Sundararajan et al. [2017].

Specifically, let the input image  $\mathbf{x} \in \mathbb{R}^n$  be divided into the foreground region  $\mathbf{x}^{\text{fg}} \in \mathbb{R}^{n^{\text{fg}}}$  and the background region  $\mathbf{x}^{\text{bg}} \in \mathbb{R}^{n^{\text{bg}}}$ , where  $n = n^{\text{fg}} + n^{\text{bg}}$  and  $\mathbf{x} = \mathbf{x}^{\text{fg}} \sqcup \mathbf{x}^{\text{bg}}$ . The foreground region  $\mathbf{x}^{\text{fg}}$  consisted of all pixels covered by the annotated semantic parts in Section B.2, and the background region  $\mathbf{x}^{\text{bg}}$  consisted of all other uncovered pixels. Let  $\mathbf{b}^{\text{bg}} \in \mathbb{R}^{n^{\text{bg}}}$  denote the baseline value for pixels in the background region  $\mathbf{x}^{\text{bg}} \in \mathbb{R}^{n^{\text{bg}}}$ . We defined the background region  $\mathbf{x}_{\alpha}^{\text{bg}}$  with strength  $\alpha$  w.r.t. the baseline value  $\mathbf{b}^{\text{bg}}$  as  $\mathbf{x}_{\alpha}^{\text{bg}} = \alpha \cdot \mathbf{x}^{\text{bg}} + (1 - \alpha) \cdot \mathbf{b}^{\text{bg}}$ , where the strength  $\alpha \in [0, 1]$ . When  $\alpha = 0$ , the background region was masked by the baseline value, i.e.  $\mathbf{x}_{\alpha=0}^{\text{bg}} = \mathbf{b}^{\text{bg}}$ . When  $\alpha = 1$ , the background region remained its original value, i.e.  $\mathbf{x}_{\alpha=1}^{\text{bg}} = \mathbf{x}^{\text{bg}}$ . When we computed the effect of each interaction concept  $S$ , we averaged the interaction effect when we were given multiple background regions with different strengths  $\alpha$ , as follows.

$$I(S|\mathbf{x}) = \mathbb{E}_{\alpha \sim \mathcal{U}[0, 1]} \left[ I \left( S \mid \mathbf{x}^{\text{fg}} \sqcup \mathbf{x}_{\alpha}^{\text{bg}} \right) \right] = \int_0^1 I \left( S \mid \mathbf{x}^{\text{fg}} \sqcup \mathbf{x}_{\alpha}^{\text{bg}} \right) d\alpha \quad (3)$$

### B.5. The eight sub-categories in the *tic-tac-toe* dataset

In this section, we provide more details on the eight sub-categories for positive samples in the *tic-tac-toe* dataset, as mentioned in the footnote<sup>4</sup> of the paper.

Each sample  $\mathbf{x}$  in the *tic-tac-toe* dataset Dua and Graff [2017] encodes one possible board configurations at the end of tic-tac-toe games. Specifically, each variable  $\mathbf{x}_i$  indicates the state at the  $i$ -th position of the board, where  $\mathbf{x}_i = 1$  indicates the player “X” has taken this position,  $\mathbf{x}_i = -1$  indicates the player “O” has taken this position, and  $\mathbf{x}_i = 0$  indicates this position is blank. If one of the player in the tic-tac-toe game creates a “three-in-a-row”, then this player wins the game. In the *tic-tac-toe* dataset, positive samples includes all configurations where the player “X” wins the game. Since there are eight possible ways for the player “X” to create a “three-in-a-row”, there are eight corresponding sub-categories for positive samples in the *tic-tac-toe* dataset. Specifically, these sub-categories contain patterns  $\mathbf{x}_1 = \mathbf{x}_2 = \mathbf{x}_3 = 1$  (three-in-the-first-row),  $\mathbf{x}_4 = \mathbf{x}_5 = \mathbf{x}_6 = 1$  (three-in-the-second-row),  $\mathbf{x}_7 = \mathbf{x}_8 = \mathbf{x}_9 = 1$  (three-in-the-third-row),  $\mathbf{x}_1 = \mathbf{x}_4 = \mathbf{x}_7 = 1$  (three-in-the-first-

column),  $x_2 = x_5 = x_8 = 1$  (three-in-the-second-column),  $x_3 = x_6 = x_9 = 1$  (three-in-the-third-column),  $x_1 = x_5 = x_9 = 1$  (three-in-the-main-diagonal),  $x_3 = x_5 = x_7 = 1$  (three-in-the-anti-diagonal), respectively.

## C. More experimental results

### C.1. More visualization of interaction concepts

This section provides more visualization of interaction concepts, as a supplement to Fig. 1 and Fig. 2 of the paper. Specifically, Fig. 15 and Fig. 16 show interaction concepts  $S$  encoded by two ResMLP-5 networks trained on the *wifi* dataset and the *tic-tac-toe* dataset, respectively. Fig. 17 shows interaction concepts  $S$  encoded by PointNet++ trained on the ShapeNet dataset. Fig. 15, 16, and 17 also show histograms of effects  $I(S|\mathbf{x})$  over different samples<sup>4</sup>, where  $S$  was extracted as a salient concept. We found that the same interaction concept usually made similar effects on different samples. This supported the conclusion in Section 3.3.2, *i.e.* the DNN usually learned transferable concepts over different samples.

### C.2. More verification on the existence of a concept dictionary

As a supplement to Fig. 4, Section 3.3.2 of the paper, we conducted another experiment to show the existence of a small concept dictionary  $\mathbf{D}_k$  that could explain most concepts encoded by the DNN. Different from the experiment in Section 3.3.2, we extracted salient concepts  $\Omega_{\mathbf{x}}$  by using the vanilla threshold  $\tau = 0.05 \cdot \max_S |I(S|\mathbf{x})|$ . Fig. 14 shows that there usually existed a concept dictionary consisting of 40-150 concepts, which could explain more than 60%-80% salient concepts encoded by the DNN. This still verified that the DNN learned transferable concepts over different samples.

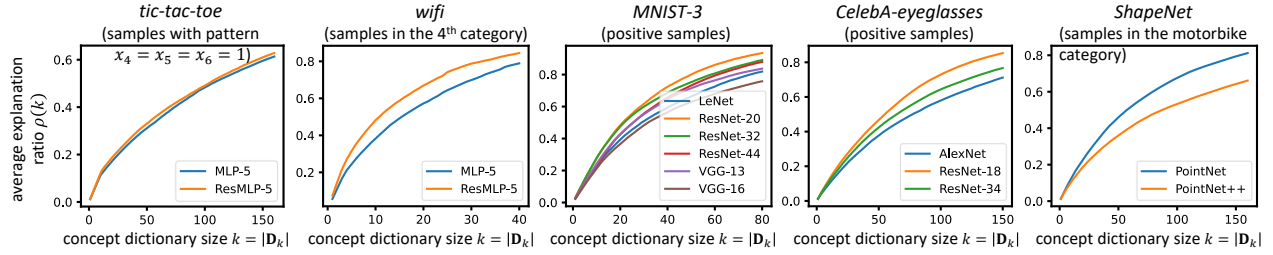


Figure 14. The change of the average explanation ratio  $\rho(k)$  along with the size  $k$  of the concept dictionary  $\mathbf{D}_k$ , when we extracted salient concepts using the vanilla threshold  $\tau = 0.05 \cdot \max_S |I(S|\mathbf{x})|$ .

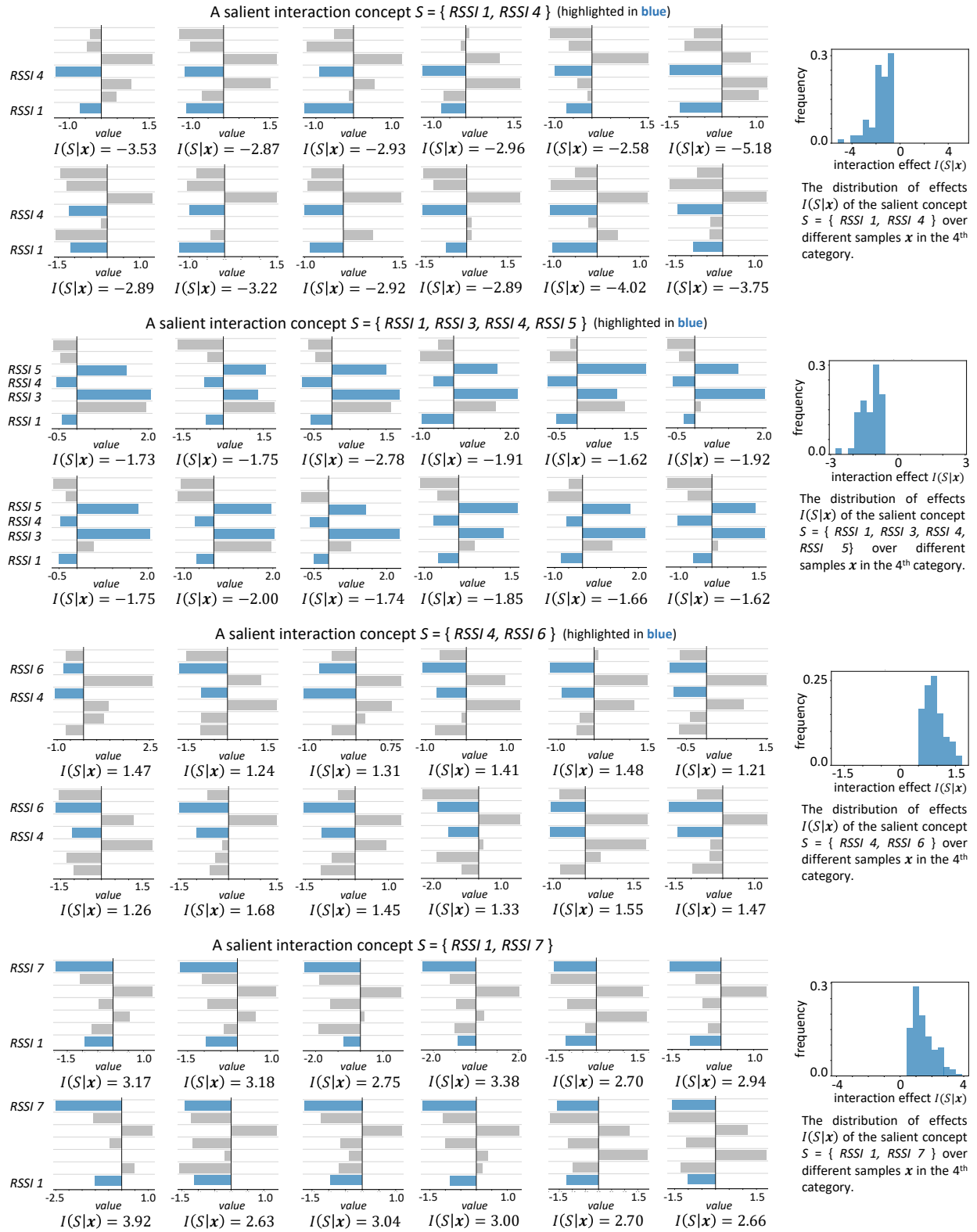


Figure 15. Visualization of salient interaction concepts  $S$  extracted by the ResMLP-5 network on different samples in the *wifi* dataset.

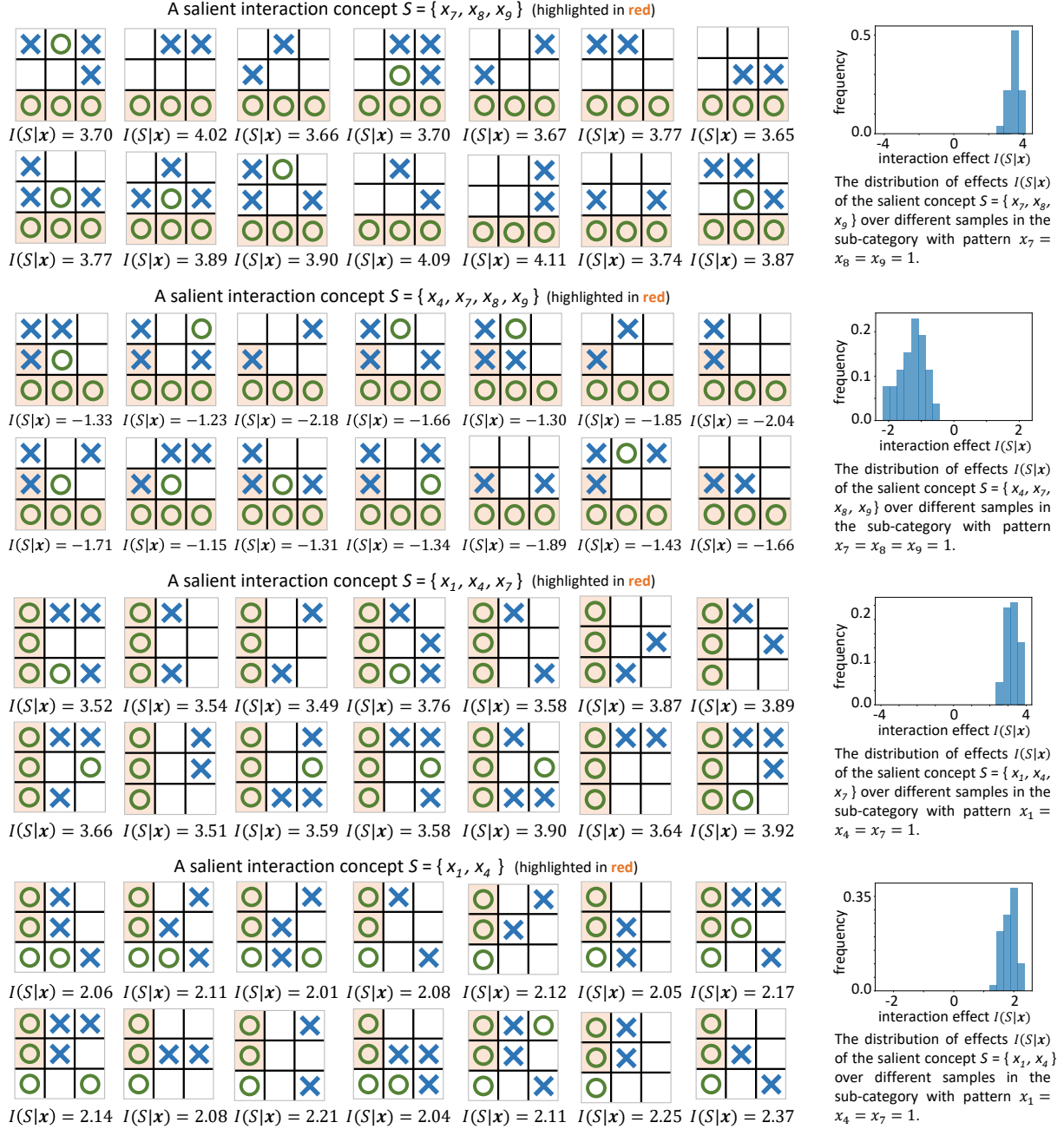


Figure 16. Visualization of salient interaction concepts  $S$  extracted by the ResMLP-5 network on different samples in the *tic-tac-toe* dataset.

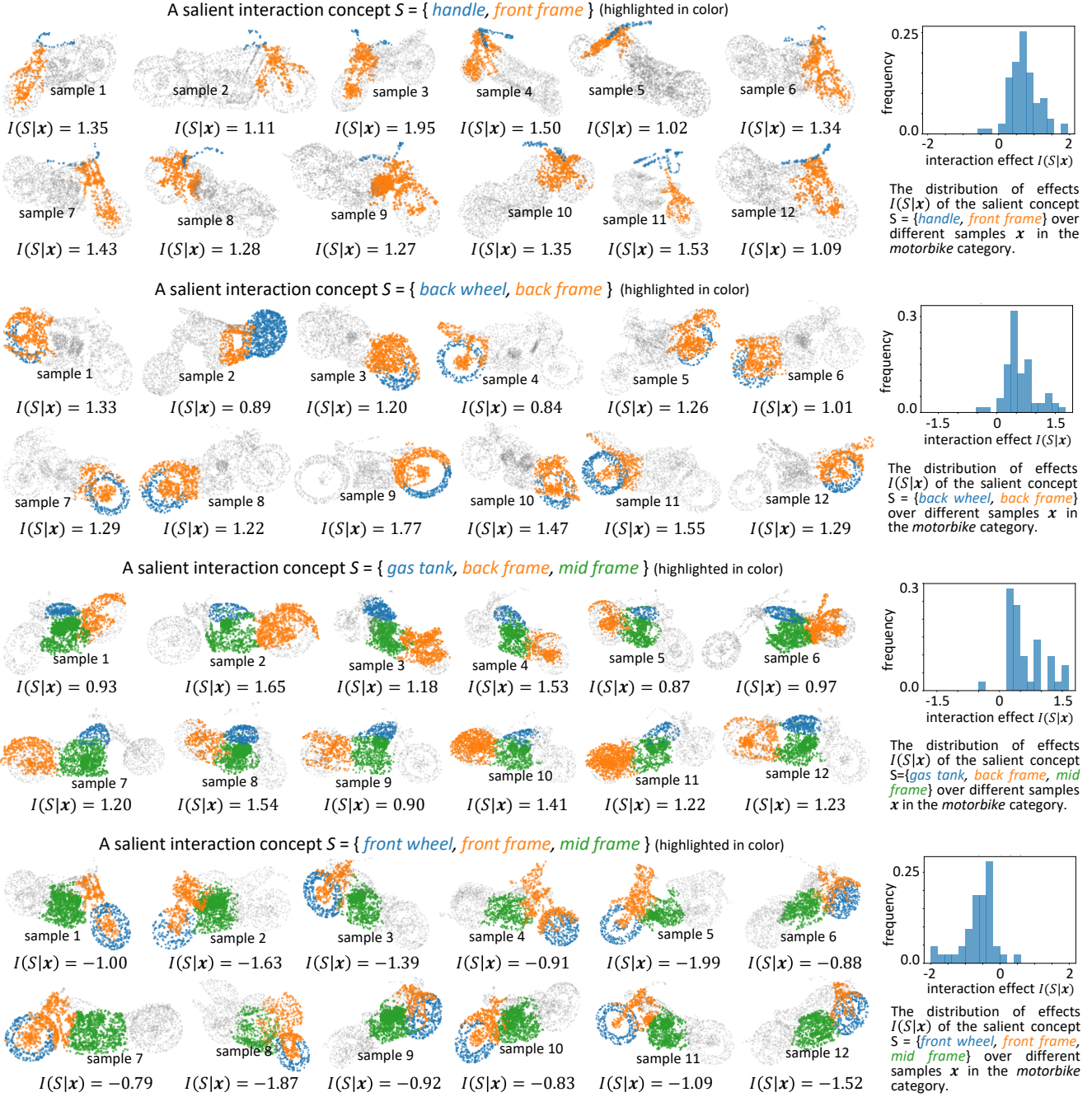


Figure 17. Visualization of salient interaction concepts  $S$  extracted by the PointNet++ network on different samples in the ShapeNet dataset.